M.O. Haluschak[1], S.I. Mudryi[2], M.A. Lopyanko[3], S.V. Optasyuk[4], T.O. Semko[3], L.I. Nikiruy[3], I.V. Horichok[3]

[1]Ivano-Frankivsk National Technical University of Oil and Gas,
15, Karpatska St., Ivano-Frankivsk, 76018, Ukraine;
[2]I.Franko National University of Lviv,
6, Kyrylo and Mefodiy St., Lviv, 79005, Ukraine;
[3]V.Stefanyk Precarpathian National University,
57, Shevchenko St., Ivano-Frankivsk, 76018, Ukraine;
[4] Kamyanets-Podilsky State University,
61, I.Ohienko St., Kamyanets-Podilsky, 32300, Ukraine

PHASE COMPOSITION AND THERMOELECTRIC PROPERTIES OF MATERIALS IN *Pb-Ag-Te* SYSTEM

The phase composition and thermoelectric properties of silver doped lead telluride with impurity concentration 0.3, 0.5, 1.0 at. % and of $Pb_{18-x}Ag_2Te_{20}$ (x = 0, 0.5, 1.0) and $Pb_{17}Ag_3Te_{20}$. solid solutions were investigated. It was established that Pb phase exists in the samples on doping, and Te and $Ag_{10.6}Te_7$ exist in solid solutions. All materials under study are characterized by high values of the Seebeck coefficient (> 300 μV/K), and the samples of solid solutions, in addition, exhibit low thermal conductivity (≈ 0.003 W/(cm·K)).

Key words: lead telluride, doping, solid solutions, thermoelectric properties.

Introduction

In recent years, considerable gain in thermoelectric figure of merit of materials based on lead telluride has been achieved due to creation of a new class of $Ag_xPb_mSb_{2-x}Te_{m+2}$ (LAST) compounds [1 – 5]. The atoms of silver and antimony in these materials occupy positions in the cation sublattice, and, since the former is acceptor and the latter – donor, they compensate the electric action of each other, without having a significant impact on carrier concentration. However, nanosize violations of crystal lattice periodicity created in the regions rich in *Ag* and *Sb* effectively scatter phonons which results in considerable reduction of thermal conductivity. Despite the large number of papers dedicated to four-component systems, the properties of materials in *Pb-Ag-Te* system are much less studied. However, such studies can serve the basis for further modification of thermoelectric characteristics of LAST four-component systems.

Silver impurity in lead telluride can exhibit both acceptor properties, substituting for lead atoms, and donor properties, being arranged in the interstitial voids [6]. This fact complicates obtaining of *PbTe*: *Ag* material with the assigned conductivity, and therefore in practice for obtaining of *p*-type conductivity material silver is not often used. Instead, such acceptor impurities as sodium and thallium are much more actively studied and used in practice. However, the use of *Na* or *Tl* is involved with a number of problems, since thallium is rather toxic, and sodium is exceptionally sensitive to the conditions of storage and use. Thus, silver can be an alternative to the aforementioned materials that are used for obtaining of *p-PbTe*.

Structural and thermodynamic properties of *Pb-Te-Ag* system were studied in [7 – 9]. Silver with tellurium forms a number of refractory compounds which must be taken into account in the synthesis. In [10], based on ab initio calculations, it was established that silver substituted for lead in cation site increases considerably the density of states at the edge of the valence band, which contributes to growth of the Seebeck coefficient. The electrophysical properties of *PbTe-Ag* were studied in [12 – 14]. Based on their analysis we can conclude that the electric activity of impurity is largely determined by the conditions for obtaining a prototype. Thus, at impurity concentration 0.5 at. % carrier concentration achieved in [12] was $\approx 2 \cdot 10^{18}$ cm^{-3}, and in [13] – $\approx 10^{19}$ cm^{-3}. So, to establish factors affecting the behaviour of *Ag* impurity is the task of vital importance.

In this paper, when choosing chemical compositions of doped samples, the goal was to study both homogeneous samples and at the interface of and beyond the impurity solubility region. In the case of solid solutions compositions were selected in the vicinity of LAST-18 ($Pb_{18}Ag_1Sb_1Te_{20}$) system as one of the most promising thermoelectric materials, and lead content was varied in addition with a view to control metal vacancies concentration in order to increase the electric conductivity of samples.

Experimental procedure

Synthesis of materials was performed in quartz ampoules evacuated to residual pressure 10^{-4} Pa. Use was made of substances with the content of basic component 99.99 % (metals and chalcogens) which were subject to additional purification. Weighing was performed on the analytical balance VLR-200M to an accuracy of 0.05 mg. To increase the homogeneity of compounds in the process of synthesis, they were subject to forced mixing. Cooling was done at a rate of 5 K/h to temperature 600 °C, and subsequently – at a rate of 10 °C/h.

The obtained ingots were ground in agate mortar and, on separation of fractions (0.05 – 0.5) mm, were pressed under 1.5 GPa. The resulting cylinder-shaped samples with $d = (5 – 8)$ mm and $h \approx (8 – 12)$ mm were annealed in the air at temperature $T = 500$ K for 5 hours.

Phase composition and structure of synthesized ingots and samples were studied by X-ray diffraction methods on automatic diffractometer STOE STADI P (manufactured by "STOE & Cie GmbH", Germany). Processing of the experimental diffraction arrays was performed by means of software packages STOE WinXPOW (version 3.03) and PowderCell (version 2.4). Refinement of crystalline structure of phases for selected samples in the isotropic approximation for atomic displacement parameters was performed by the Rietveld method using FullProf. 2 k program (version 5.30).

The Hall measurements were performed in constant magnetic and electric fields by the four-probe method. Current through the samples was $\approx 100 – 500$ mA. The magnetic field was directed perpendicular to the longitudinal axis of cylinder sample at induction 1.5 T.

The Seebeck coefficient α, electric conductivity σ and thermal conductivity *k* were determined by the methods described in [15, 16].

Discussion of the results

The results of X-ray diffraction studies are represented in Table and in Fig. 1. Samples of undoped material are single-phase and characterized by *n*-type conductivity. On introduction of impurity, traces of pure lead phase become apparent (Fig. 1 *b*).

Table

Results of X-ray diffraction analysis and measurement of the Hall effect (at room temperatures) of pressed and annealed samples of PbTe: Ag and $Pb_{18-x-y}Ag_xTe_{20}$

Sample	Chemical composition	Phase composition	Unit cell parameter a, Å[1]	Carrier concentration $n(p)$, cm^{-3}
15 – 18 2*S*	$Pb_{0.5}Te_{0.5}$	*PbTe*	6.4565	$4.9\ 10^{18}$
15 – 22 1*S*	$Pb_{0.5}Te_{0.5}$+0.3 at.% *Ag*	*PbTe*, traces of *Pb*	6.4561	$8.46\ 10^{17}$
15 – 23 1*S*	$Pb_{0.5}Te_{0.5}$+0.5 at.% *Ag*	*PbTe*, traces of *Pb*	6.4571	$1.2\ 10^{18}$
15 – 21 1*S*	$Pb_{0.5}Te_{0.5}$+1.0 at.% *Ag*	*PbTe*, traces of *Pb*	6.4552	$6.4\ 10^{17}$
16 – 13 2*S*	$Pb_{18}Ag_2Te_{20}$	*PbTe*, traces of $Ag_{10.6}Te_7$	6.4571	$1.4\ 10^{18}$
16 – 14 2*S*	$Pb_{17.5}Ag_2Te_{20}$	*PbTe*, traces of *Te* and $Ag_{10.6}Te_7$	6.4582	$1.2\ 10^{18}$
16 – 15 1*S*	$Pb_{17.0}Ag_2Te_{20}$	*PbTe*, traces of *Te* and $Ag_{10.6}Te_7$	6.4576	$1.3\ 10^{18}$
XIX	$Pb_{17}Ag_3Te_{20}$	*PbTe*, traces of *Te* and $Ag_{10.6}Te_7$	6.4592	$1.1\ 10^{18}$

[1]Note. Absolute error is ± 0.0005

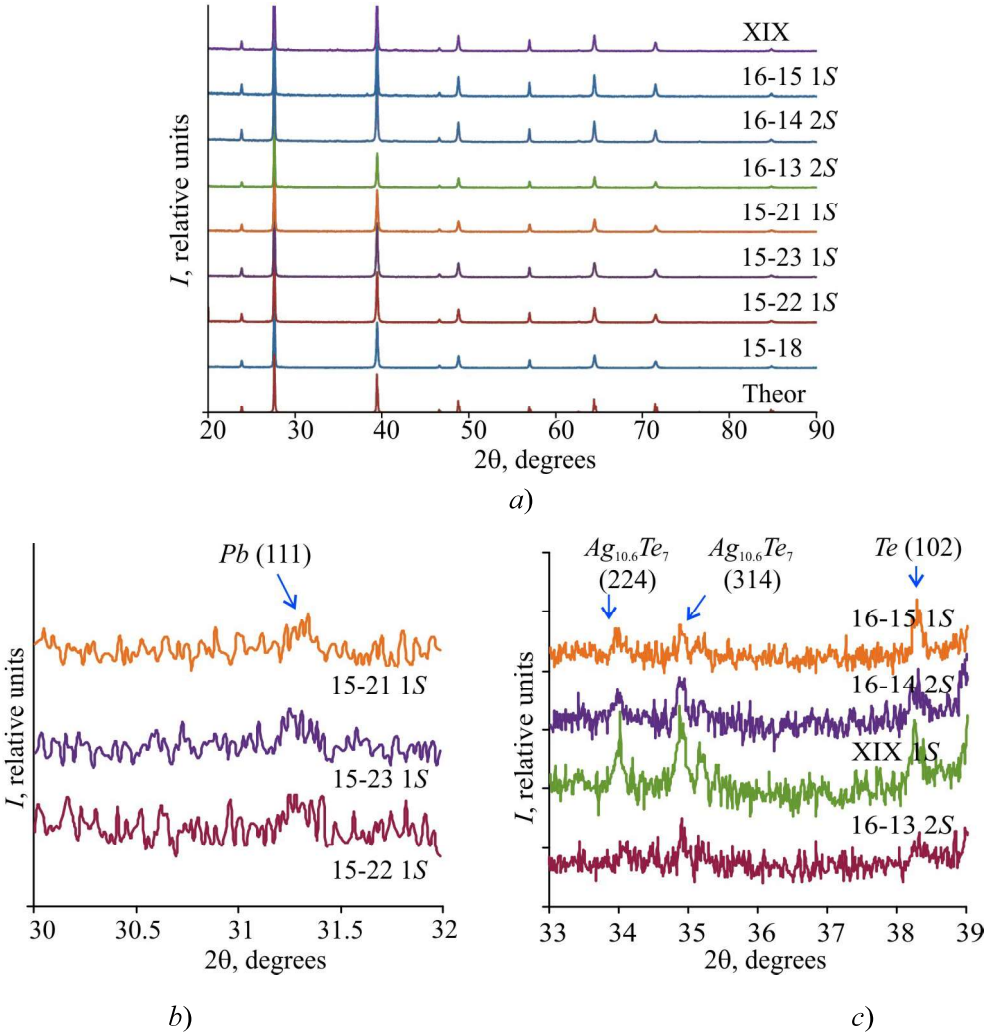

Fig. 1. X-ray patterns of Pb-Ag-Te samples under investigation (see Table 1) (a) and X-ray pattern fragments in the area of detected Pb phase reflexes for doped PbTe: Ag (b) and Te and $Ag_{10.6}Te_7$ phases for PbAgTe solid solutions (c).

For $Pb_{18}Ag_2Te_{20}$, $Pb_{17.5}Ag_2Te_{20}$, $Pb_{17.0}Ag_2Te_{20}$ solid solutions the lattice constant and carrier concentration are practically equal, and for a sample of $Pb_{17}Ag_3Te_{20}$ composition the lattice constant is greater. For all samples of *Pb-Ag-Te* solid solutions on X-ray diffraction patterns there is an additional phase of *Te* and $Ag_{10.6}Te_7$ (Fig. 1 *b*) [17]. The latter is due to over limits of impurity solubility region, and the former – due to considerable excess of chalcogen in the charge as compared to stoichiometric composition.

Silver doping results in considerable reduction of electric conductivity (Fig. 2 *a*), but no *p*-type transition takes place. The Seebeck coefficient of samples with impurity content 0.3 and 0.5 at. % *Ag* is almost the same and monotonically decreases from the values 500 μV/K at 100 °C to the values 350 μV/K at 350 °C. The temperature dependence of the Seebeck coefficient of samples with impurity content 1 at. % *Ag* is characterized by nonmonotonic behaviour with the maximum 400 μV/K at 200 °C. The thermal conductivity coefficient weakly grows with increase in impurity amount.

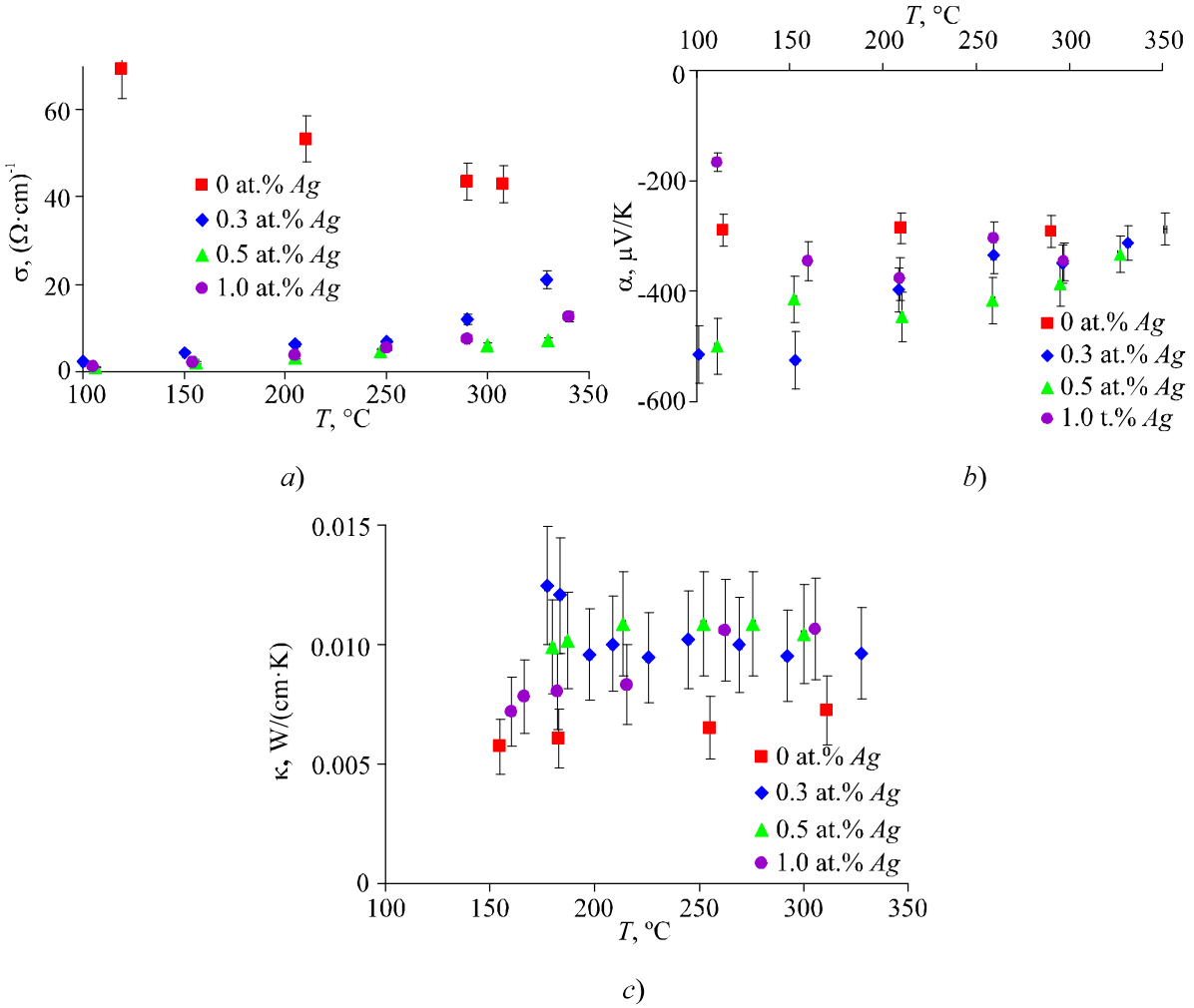

Fig. 2. Temperature dependences of electric conductivity σ (a), the Seebeck coefficient α (b) and thermal conductivity coefficient k (c) of PbTe (■), PbTe: Ag (0.3 at. %) (●), PbTe: Ag (0.5 at. %) (▲), PbTe: Ag (1.0 at. %) (♦) samples.

Unlike doped material, a stable *p*-type conductivity was obtained for all $Pb_{18-x}Ag_{2(3)}Te_{20}$ (x = 0; 0.5; 1.0) compositions under study. From Fig. 3 *a* it is seen that material has higher electric conductivity as compared to doped material. There is a marked increase in σ value with a decrease of

lead content in solution, though according to the Hall measurements, carrier concentration is practically unchanged (Table). The Seebeck coefficient for all $Pb_{18-x}Ag_2Te_{20}$ compositions is almost the same and makes ≈ 300 μV/°C at 300 °C. The thermal conductivity coefficient is reduced with decreasing content of lead in solution, which is attributable to increased number of lead vacancies on which phonons are scattered. The lowest k value is typical of samples with $Pb_{17}Ag_3Te_{20}$ composition. It is important that the peaks of additional $Ag_{10.6}Te_7$ phase are most intensive for the sample.

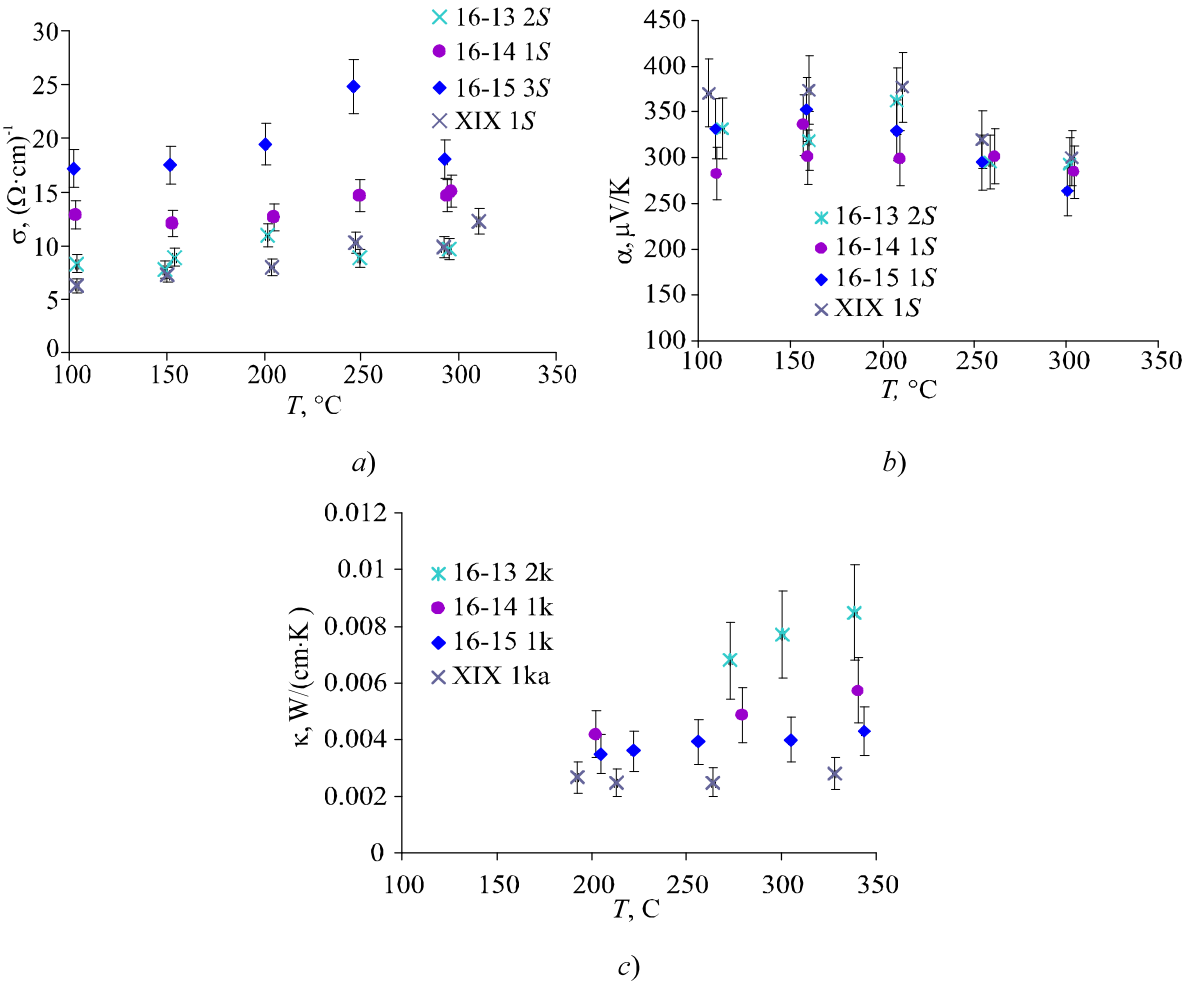

Fig. 3. Temperature dependences of electric conductivity σ (a), the Seebeck coefficient α (b) and thermal conductivity coefficient k (c) of $Pb_{18}Ag_2Te_{20}$ (×), $Pb_{17.5}Ag_2Te_{20}$(●), $Pb_{17.0}Ag_2Te_{20}$(♦) samples.

Thus, one can state a weak acceptor effect of silver in *PbTe*, to investigate into the reasons of which it is necessary to perform crystallochemical or thermodynamic analysis of defective subsystem. However, for doped *PbTe*: *Ag* material on the basis of established growth of lattice constant with increase in *Ag* content and appearance of traces of pure lead phase, an assumption can be made on silver substitution for lead atoms, by their displacement into interstices with subsequent precipitation. As long as interstitial lead atom is a double donor, and silver atom in the cation site – a single acceptor, it can account for a weak acceptor effect of silver and impossibility of material converting into *p*-type conductivity. In the case of solid solutions the electrophysical effect of silver is more pronounced as compared to doped material. Moreover, inclusions of additional phases reduce the thermal conductivity considerably, which is important from practical standpoint.

Conclusions

1. Silver impurity in lead telluride shows a weak acceptor effect, the concentration of acceptor defects is considerably lower than the concentration of introduced *Ag* atoms, and the most probable doping mechanism is substitution of silver atoms in crystal lattice for lead atoms. Doped material is characterized by high values of the Seebeck coefficient (≈ 500 μV/K at. 0.3 – 0.5 at. % *Ag*), which can be used for creation of bolometers on its basis.
2. $Pb_{18}Ag_2Te_{20}$, $Pb_{17.5}Ag_2Te_{20}$, $Pb_{17.0}Ag_2Te_{20}$ and $Pb_{17}Ag_3Te_{20}$ solid solutions are characterized by the presence of inclusions of additional *Te* and $Ag_{10.6}Te_7$ phases which determine low values of thermal conductivity (0.003 W/(cm · K)) and high in a wide range values of the Sebeck coefficient (≈ 300 μV/K), which is necessary for practical use of material in thermoelectric converters.

References

1. K-F. Hsu, S.Loo, F.Guo, W.Chen, J.S.Dyck, C.Uher, T.Hogan, E.K.Polychroniadis, and M.G.Kanatzidis, *Science* **303** (5659), 818 (2004).
2. H.Hazama, U.Mizutani, *Phys. Rev. B* 73, 115108 (2006).
3. E.Quarez, K.-F.Hsu, R.Pcionek, N.Frangis, E.K.Polychroniadis, and M.G.Kanatzidis, *J. Am.Chem. Soc*. 127, 9177 (2005).
4. J.Sootsman, R.Pcionek, H.Kong, C.Uher and M.G.Kanatzidis, *Mater. Res. Soc. Symp. Proc*. 886, 0886-F08-05 (2006).
5. D.Bilc, S.D.Mahanti, E.Quarez, K.-F.Hsu, R.Pcionek, and M.G.Kanatzidis, *Phys. Rev. Lett.* 93, 146403 (2004).
6. B.A.Volkov, L.I.Ryabova, and D.R.Khokhlov, *Advances in Physical Sciences* **178** (8), 875 (2002).
7. W.Gierlotka, J.Lapsa, and K.Fitzner, *J. Phase Equilibria and Diffusion* **31** (6), 509 (2010).
8. M.K.Sharov, *Inorganic Materials* **44** (6), 569 (2008).
9. M.K.Sharov, *Russian Journal of Inorganic Chemistry* **54** (1), 33 (2009).
10. K.Hoang, D.Mahanti, and P.Jena, *Phys Rev B* 76, 115432 (2007).
11. A.V.Dmitriev, I.P.Zviagin, *Advances in Physical Sciences* **180** (8), 821 (2010).
12. M.K.Sharov, *Semiconductors* **46** (5), 613 (2012).
13. L.D.Borisova, *Phys. Stat. Sol. A* 53, K19 (1979).
14. H.S.Dow, M.W.Oh, B.S.Kim, S.D.Park, B.K.Min, H.W.Lee, and D.M.Wee, *J.Applied Physics* 108, 1137709 (2010).
15. D.M.Freik, C.A.Kryskov, I.V.Horichok, T.S.Lyuba, O.S.Krynytsky, and O.M.Rachkovsky, *J.Thermoelectricity* 2, 42 (2013).
16. D.M.Freik, R.Ya.Mykhailyonka, and V.M.Klanichka, *Physics and Chemistry of Solid State* **5** (1), 173 (2004).
17. J.Peters, O.Conrad, B.Bremer, and B.Z.Krebs, *Z. Anorg. Allg. Chem*. 622, 1823 (1996).

Submitted 27.06.2016.

L.I. Anatychuk[1,2], R.V. Kuz[1]

[1]Institute of Thermoelectricity, 1, Nauky Str.,
Chernivtsi, 58029, Ukraine;
[2]Yu.Fedkovych Chernivtsi National University
2, Kotsyubinsky str., Chernivtsi, 58012 Ukraine

L.I. Anatychuk

R.V. Kuz

THERMOELECTRIC GENERATOR FOR TRUCKS

The results of computer simulation of thermoelectric generators (TEG) using the exhaust heat of internal combustion engines were presented. The simulation was done with regard to dynamic modes of engine operation on the basis of real records of monitoring system with the use of real parameters of thermoelectric modules.

Key words: thermoelectric generator, internal combustion engines.

Introduction

The use of waste heat from the internal combustion engines is one of the critical tasks of thermoelectricity. World producers of vehicles, as well as companies of thermoelectric profile, give much prominence to the development of efficient automotive thermoelectric generators [1 – 8]. The purpose is to increase fuel saving up to 10 % due to the use of engine exhaust heat for electric energy generation.

The largest companies making it their mission to create industrial prototypes of generators and their large-scale production are Hi-Z, BSST and General Motors in the USA. In Japan, the problems of creating automotive generators are most widely addressed by companies Komatsu, Nissan and Shiroki. In Germany, company Volkswagen and company BMW together with DLR (German Airspace Centre) represented their developments of thermoelectric automotive generators.

The lack of broad application of automotive TEG is attributable to insufficiently high generator efficiency. The generator efficiency essentially depends on the engine operating mode. The dynamic modes of engine operation during an actual drive impose fairly complicated requirements to design and optimization of automotive generators that cannot be fully met so far. One of optimization components is TEG design for a specific engine type and its priority operating mode. Particular attention is claimed by trucks with heavy engines and, accordingly, large amount of exhaust heat.

The purpose of this work is to design a thermoelectric generator which utilizes the exhaust heat of truck engine.

Optimization of a thermoelectric generator is done by computer design [10] which is as follows.

Computer design procedure

Let us consider a physical model of thermoelectric generator (TEG) shown in Fig. 1. In the general case a TEG is composed of N sections connected in series with respect to hot gas flow and cold heat carrier.

Each TEG section comprises the following components (Fig. 1): hot heat exchanger (1), thermopile (3) with thermal resistance $R_t^{(i)}$ and efficiency $\eta(T_H, T_0)$; cold heat exchanger (4) with